

Surface characterisation studies of nickel–chromium PVD: EB evaporated low carbon steel samples

B. Subramanian*, M. Jayachandran and S. Jayakrishnan

Increasing concern over toxic wastes produced by nickel–chromium (Ni–Cr) plating industries has resulted in strong research efforts to replace conventional plating by physical vapour deposition techniques like evaporation and sputtering. Ni–Cr coatings on mild steel substrates produced by an electron beam evaporation process with layer thickness of $\sim 8\text{--}10\ \mu\text{m}$ have been investigated with regard to the structural and corrosion properties. The structure of the coating was evaluated by X-ray diffractometer (XRD). The (110) Cr and (200) Ni predominant peaks with the crystallite size in the range of 25–30 nm was observed from XRD pattern. The electrochemical polarisation studies performed on samples showed the corrosion resistant nature of the evaporated Cr coating with Ni underlayer on mild steel substrates. Atomic force microscopy (AFM) and scanning electron microscopy (SEM) were used to investigate the surface characteristics of the samples before and after the electrochemical corrosion tests. The localised corrosion through a micropore in the evaporated Cr deposit and its penetration to the Ni layer was observed from SEM. The smaller change in roughness observed from AFM reflects the resistance of this coating to corrosion breakdown.

Keywords: Electron beam evaporation, PVD, Accelerated corrosion tests, AFM, SEM

Introduction

In the nickel/chromium electroplating systems, the nickel plate is used principally as bright coating underneath a much thinner chromium electroplate thus providing a highly lustrous and corrosion protective finish for articles such as steel, brass and zinc based die casting.¹ Decorative nickel plating processes produce mirror bright and highly levelled deposits which improve the appearance of polished steel significantly. The degree of improvement in corrosion performance is being appreciated because modern, decorative, electroplated nickel plus chromium coatings protect steel from corrosion.² Electrodeposition of chromium–nickel compositionally modulated multilayers (CMM) from a trivalent chromium bath exhibited improved corrosion and wear resistance.³ When chromium deposits are used with nickel undercoats of suitable thickness, steel substrates can be protected for long periods of outdoor atmospheric exposure. The occurrence of localised corrosion causes the decorative appearance of the deposited article to be unacceptable.^{4,5}

Nickel and chromium deposits are usually relatively hard and their hardness generally exceeds that of the metal under the cold worked condition.⁶ High

temperature oxidation and wear of heat transfer tubes and other structural materials used in cold fired boilers are recognised as being the main causes of downtime in power generation plant, and account for 50–75% of the arrest time.⁷ Ni–Cr coatings are mainly used in order to drastically decrease the oxidation and gas corrosion of different metallic substrates.⁸

Traditional chromium deposits are produced from chemical baths containing hexavalent chromium ions (Cr^{6+}). Chromium(VI) electroplating processes produce large volumes of chromium contaminated toxic waste, air pollution and water contamination which can result in a significant induction of cytogenetic damage in electroplating workers⁹ and a clear genotoxic effect associated with occupational exposure to chromium.¹⁰

Physical vapour deposition (PVD) processes avoid pollution problems associated with electrodeposited chrome and also the hydrogen embrittlement associated with plating. The PVD coating method has the flexibility to tune the coating properties by changing composition, creating multilayers, adjusting the mechanical properties and influencing the microstructure.^{11,12}

In the present paper, the corrosion behaviour of Ni–Cr electron beam (EB) evaporated coatings was evaluated using standard three electrode electrochemical cell measurements. Surface morphology of the samples, before and after the corrosion tests, was studied through the use of scanning electron microscopy (SEM) and atomic force microscopy (AFM).

Experimental

Nickel and chromium of $\sim 10 \mu\text{m}$ thickness were sequentially EB evaporated onto ultrasonically cleaned low carbon steel substrates in a vacuum of $\sim 10^{-6}$ mbar in a vacuum coating unit (12" Hind Hi Vac). The optimised process parameters are shown in Table 1.

Coatings were analysed for crystallographic structure by a JEOL JDX 803 a X-ray diffractometer (XRD) using Cu K_{α} line. The microstructure of these coatings was examined using Hitachi S 3000H SEM and molecular imaging AFM. The Vickers' hardness of sample used in the present investigation was determined using a microhardness testing machine Leco DM 400.

The thickness of the coatings was measured using Mitutoyo profilometer. Profilometer is useful for measuring surface roughness profiles of coatings. However, they can be used to measure the step height between substrate and the adjacent coating. A stylus is drawn across the step from the substrate to the coating and both the vertical and horizontal motion of the stylus is amplified and recorded. A region of the mild steel substrate was masked before evaporating the elements.

Electrochemical polarisation studies were carried out on $10 \times 10 \times 2$ mm thick Ni-Cr coated test coupons using BAS IME electrochemical analyser. Experiments were conducted using the standard three electrode configuration, saturated calomel as a reference electrode with a platinum foil as a counter electrode and the sample as a working electrode. Specimen (0.5 cm^2 exposed area) was immersed in the test solution of 3.5% NaCl. Experiments were carried out at room temperature (25°C).

Results and discussion

Structural and microstructure analysis

The XRD patterns showed polycrystalline nature with (110) Cr and (200) Ni predominant peaks as shown in Fig. 1a for the as prepared sample.

The observed d values are in good agreement with that of standards obtained from JCPDS as listed in Table 2. The particle size D was calculated from line broadening β , under the simple assumption that line broadening is caused by the particle size alone¹²

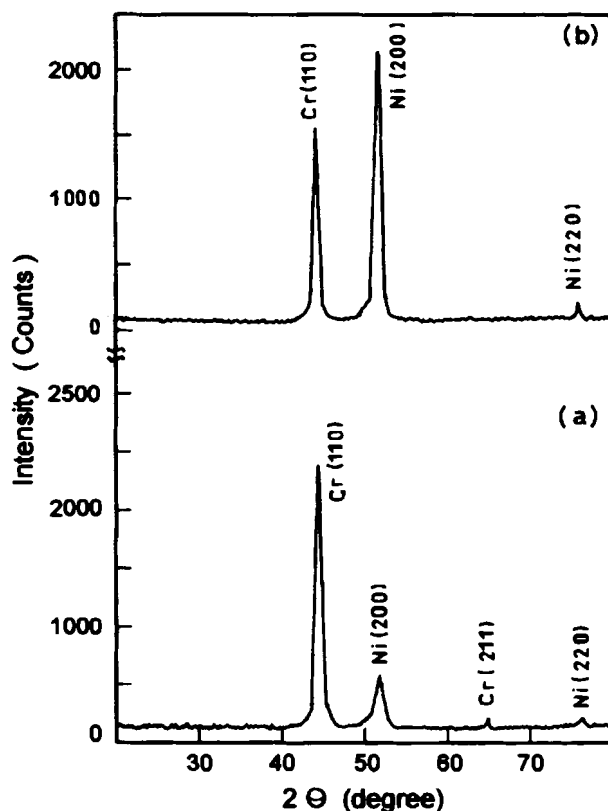
$$D = (0.9\lambda / \beta \cos \phi) \quad (1)$$

here λ is the X-ray wavelength (1.514 \AA for Cu K_{α}) and ϕ is the Bragg angle.

The crystallite sizes were determined in the range of 25–30 nm for NiCr layers on low carbon steel substrates. The XRD pattern obtained for the sample after performing the electrochemical corrosion test in 3.5% w/v NaCl solution is shown in Fig. 1b. Reduction in (110) Cr intensity and sharp rise in (200) Ni peak as

Table 1 Evaporation parameter for Ni-Cr deposition

Parameter	Optimised value
Ultimate vacuum, mbar	1×10^{-6}
Evaporant materials	Ni and Cr (purity 99.9%)
Distance between source and substrate, mm	290
Substrate temperature, $^{\circ}\text{C}$	RT 28 ± 0.5
Potential, kV	5.6
Current, mA	50
Duration of Ni evaporation, min	30
Duration of Cr evaporation, min	5



1 X-ray diffraction obtained for *a* as evaporated sample and *b* after accelerated corrosion tests in 3.5% w/v NaCl solution at 25°C

shown in Fig. 1b are due to the formation of pits and exposure of the Ni underlayer. This is because of the penetration of corrosion through micropores as observed from SEM and AFM analysis discussed later in the present paper.

Thickness and composition of coating

For the measurement of layer thickness XRF was used as a fast method, providing an estimate of the average layer thickness over an area of $\sim 2 \text{ mm}^2$ after calibration with specimens of known layer thickness. The thickness value of $10.5 \mu\text{m}$ was measured for the Ni-Cr coating prepared under optimised conditions. The thickness values of $9.1 \mu\text{m}$ for the evaporated Ni and $10.66 \mu\text{m}$ for the Cr overlay and underlying Ni were obtained using profilometer as shown in Fig. 2 which is in good agreement with the value of $10.5 \mu\text{m}$ obtained from XRF.

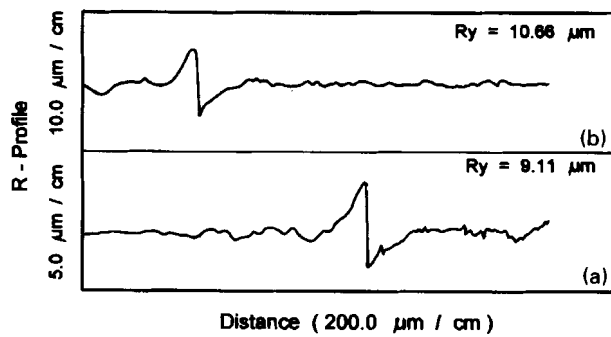
The Ni-Cr evaporated samples were bent through an angle of 180° repeatedly as required by BS 5411 standards and found no lifting or peeling which showed good adhesion of the coatings to the substrates. Figure 3 shows the XRF spectrum of the sample.

The chemical analysis of Fig. 3 gave the following composition: 71Ni-22.3Cr-3.1Fe (wt-%). The presence of Fe is due to the substrate.

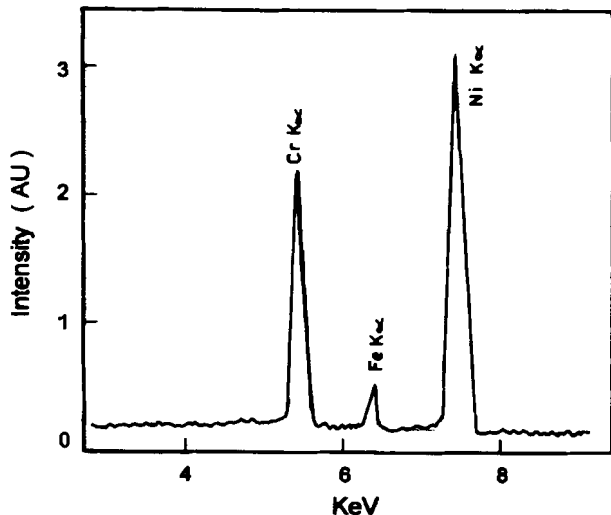
Potentiodynamic polarisation and AC impedance spectroscopy

Typical polarisation curves obtained for the corrosion behaviour of the Ni-Cr evaporated mild steel samples are shown in Fig. 4.

Table 3 includes the values of the corrosion potential E_{corr} , the corrosion current density I_{corr} , the anodic and



2 Roughness profile of *a* Ni on mild steel and *b* chromium over Ni/mild steel



3 XRF analysis of as evaporated Ni-Cr sample

cathodic Tafel slopes during polarisation in 3.5% w/v NaCl and the corrosion rate.

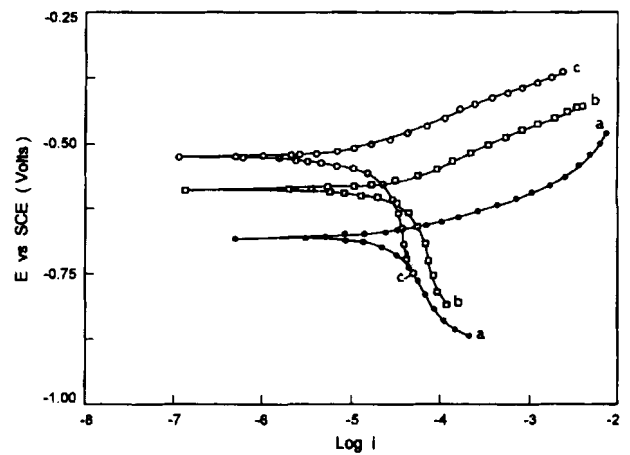
E_{corr} and I_{corr} values improve a lower negative value of E_{corr} and lower value of I_{corr} signifies an improvement in corrosion for Cr evaporation with Ni underlayer onto mild steel substrates. This may also be due to higher coating thickness which leads to a decrease in the porosity, an increase in nucleation sites and a decrease in entrapped gaseous impurities.

Table 2 Comparison of d values from XRD pattern

Samples	d_{observed} , nm	d_{standard} , nm	hkl	Relative intensity, %	Phase
As prepared sample	2.049	2.044	(110)	100.0	Cr
	1.772	1.764	(200)	19.5	Ni
	1.440	1.442	(211)	2.7	Cr
	1.250	1.240	(220)	3.26	Ni
Corrosion tested sample	2.052	2.044	(110)	71.7	Cr
	1.773	1.764	(200)	100.0	Ni
	1.254	1.240	(220)	0.99	Ni

Table 3 Corrosion parameters obtained from polarisation studies in 3.5% w/v NaCl

Sample	E_{corr} versus SCE, mV	Tafel slope		I_{corr} cathodic, mA cm ⁻²
		b_a	b_c	
		V/decade	V/decade	
Pure mild steel	-685	0.08	-0.30	8.26
Nickel on mild steel	-587	0.07	-0.53	3.94
Chromium over nickel/mild steel	-535	0.06	-0.42	1.01



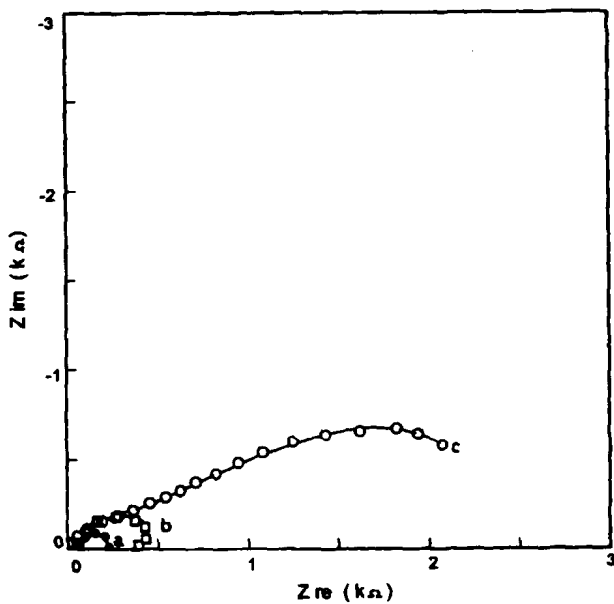
4 Polarisation studies of *a* pure mild steel, *b* nickel/mild steel and *c* chromium over nickel/mild steel in 3.5% w/v NaCl solution at 25°C

The same three electrode cell assembly, as used for the potentiodynamic polarisation experiments, was employed for the AC impedance investigations. Impedance measurements were made at open circuit potential (OCP) applying an AC signal of 10 mV in the frequency range 10 Hz–1 MHz. The Nyquist plots for the samples used for corrosion tests in 3.5% w/v NaCl solution are shown in Fig. 5.

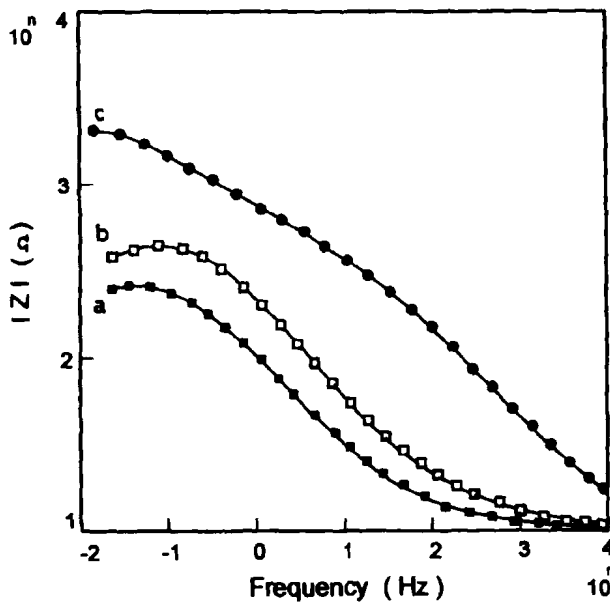
The semicircular region is more pronounced in the case of Cr evaporated sample with Ni underlayer on mild steel substrates indicating that the samples has maximum corrosion resistance as observed from the high frequency region of the impedance spectra. The same trend is also observed as shown in Fig. 6 which is the Bode plot taken for these samples. The charge transfer resistance R_{ct} and double layer capacitance C_{dl} values are given in Table 4.

It is observed that there is a notable increase in R_{ct} and a decrease in C_{dl} for the Cr evaporated mild steel sample with Ni underlayer showing that the deposit is highly corrosion resistant.

It is observed that the diffusion coefficient of the chloride ions is minimum for Cr overcoat compared with evaporated Ni and pure mild steel substrate. This



5 Nyquist plots for corrosion of *a* pure mild steel, *b* nickel/mild steel and *c* chromium over nickel/mild steel in 3.5% w/v NaCl solution at 25°C

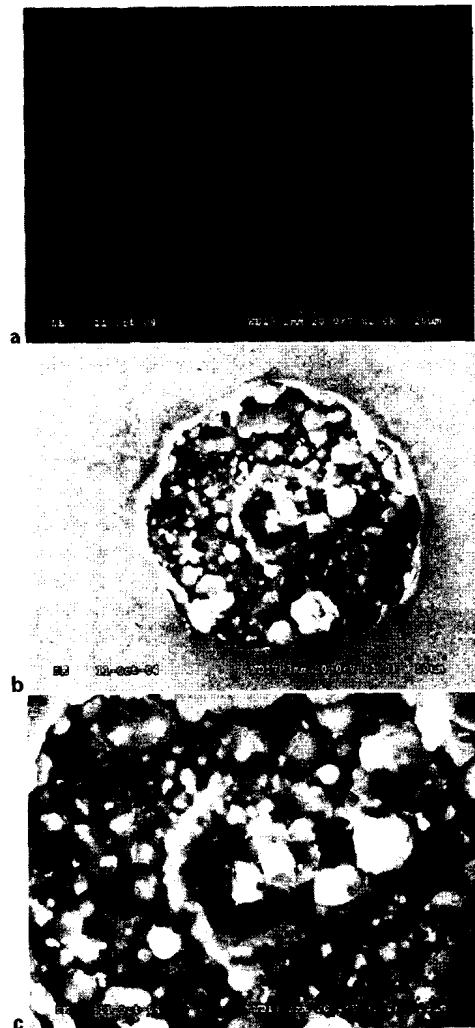


6 Bode plots for corrosion of *a* pure mild steel, *b* nickel/mild steel and *c* chromium over nickel/mild steel in 3.5% w/v NaCl solution at 25°C

trend again shows that the evaporated Cr with Ni underlayer is highly corrosion resistant.

Scanning electron microscopy surface characterisation

Using SEM, larger surface area is available for examination thereby reducing the timescale needed to examine the surface for surface damage compared with



7 Images (SEM) showing *a* as evaporated sample and *b* after accelerated corrosion tests in 3.5% w/v NaCl solution at 25°C

AFM. The surface of as prepared Ni-Cr sample is shown in Fig. 7*a*.

Fine grain structure with few microcracks on the surface was observed. When observing the corroded surface of evaporated sample, the majority of the surface was unaffected by the accelerated corrosion test in 3.5% w/v NaCl solution and only a few isolated pits having diameters ~60–80 μm were found as shown in Fig. 7*b*. Here localised corrosion has taken place through a micropore in the evaporated Cr deposit where corrosion penetrates to the Ni layer and then spreads laterally. A closer observation of this pit is shown in Fig. 7*c*.

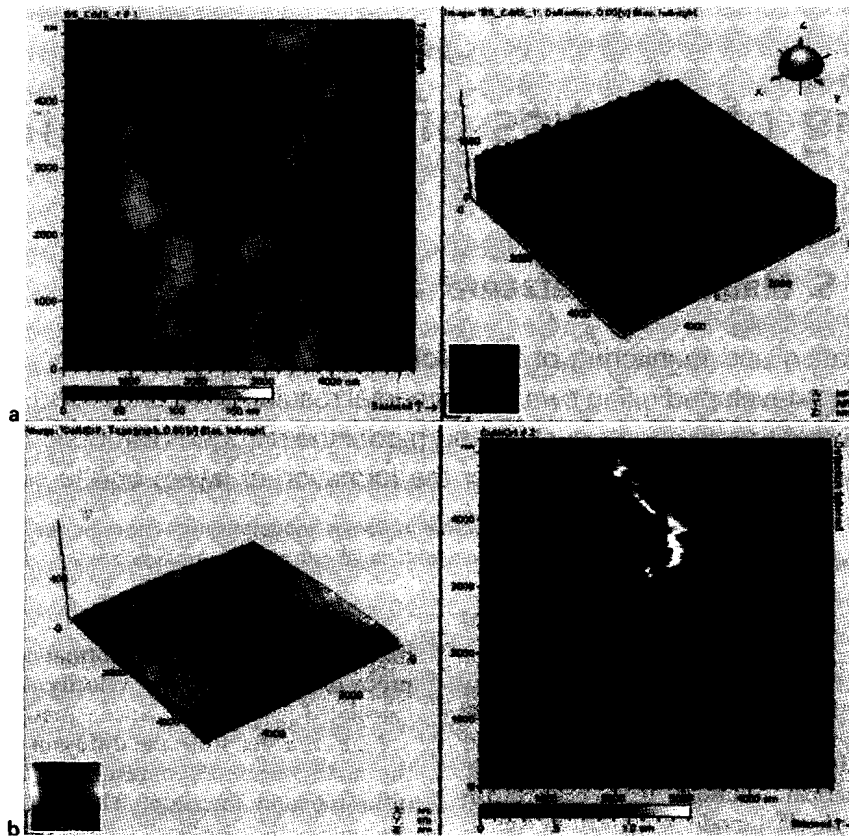
Pits or blisters containing corrosion products lead to the removal of the deposits and the formation of deep craters.

Atomic force microscopy surface analysis

Figure 8 shows the representative AFM scans over an area of 5 × 5 μm on EB evaporated Ni-Cr coatings before and after accelerated electrochemical corrosion

Table 4 Corrosion parameters obtained from impedance measurements by Nyquist plots

Sample	OCP versus SCE, mV	R_{ct} , $\Omega \text{ cm}^2$	C_{dl} , Farads cm^{-2}
Mild steel panel	-674	246	5.12×10^{-3}
Nickel on mild steel	-590	510	6.11×10^{-4}
Chromium over nickel/mild steel	-530	2500	8.01×10^{-5}



8 Images (AFM) (scan size $5 \times 5 \mu\text{m}$) showing topography of mild steel substrate of *a* as evaporated sample and *b* after accelerated corrosion tests in 3.5% w/v NaCl solution at 25°C

Table 5 Hardness and RMS roughness of samples

Test sample	Hardness	RMS roughness, nm	
		Before corrosion tests	After corrosion tests
MS substrate	360	11.5	32.0
As prepared Ni-Cr sample	489	6.3	9.2

tests. The as evaporated sample revealed no visible damage on the surface as shown in Fig. 8a.

The observation of sample following accelerated corrosion testing revealed few pits and the AFM morphology of a typical pit on the surface is shown in Fig. 8b.

The localised pitting corrosion is the method of attack.¹³ The propagation of this pit may finally coalesced to form large and deep craters resulting in the eventual failure of the deposit.

Root mean square (RMS) roughness of the sample following accelerated corrosion testing was found to increase slightly whereas a greater change in roughness value was observed for mild steel substrate as shown in Table 5. Also a considerable change in hardness was observed for these coatings on mild steel substrates.

The smaller change in RMS roughness for the evaporated Ni-Cr sample reflects the resistance of this coating to corrosion breakdown.

Conclusion

Strongly adherent Ni-Cr deposits were evaporated onto mild steel substrates. The morphology of the as evaporated and accelerated corrosion tested samples was examined by SEM and AFM. The increase in roughness for the samples after the corrosion tests was

attributed to the pit formation. The electrochemical polarisation studies performed on the evaporated Cr coating with Ni underlayer on mild steel substrates showed higher corrosion resistance than the corrosion resistance values for bare mild steel as well as nickel coated mild steel surface.

References

1. H. Xu, R. Akid and G. Brumpton: *Trans. Inst. Met. Finl.*, 2004, **82**, (1-2), 18.
2. G. A. Di Bari and R. A. Covert: *Met. Fin.*, 1990, **88**, (4), 59.
3. A. Rousean and P. Benaben, *Plating and Surf. Fin.*, 1999, **86**, (9), 106.
4. Sobha Jayakrishnan, K. Dhayanand, R. M. Krishnan, R. Sekar and S. Sriveeraraghavan, *Trans and Inst. Met. Fin.*, 1998, **70**, (3), 90.
5. D. Snyder, *Met. Fin.*, 2000, **98**, (1), 215.
6. M. E. Bahrololoom and A. Hoveidaei: *Surf. Engg.*, 1999, **15**, (6), 502.
7. V. Hignera thidalgo, J. Belzurice Varela, J. Martinez de la celle and A. Carriles Menendez: *Surf. Engg.*, 2000, **16**, (2), 137.
8. C. Panagopoulus, A. Kotsomichatis and H. Badekas: *Surf. Coat. Tech.*, 1990, **41**, 343.
9. F. Wu, W. Wn, H. Kno, C. Liu, R. Wang and J. Lai: *Sci. Tot. Env.*, 2001, **279**, 21.
10. A. Vaglenov, M. Nosko, R. Georgiena, E. Carbonell, A. Creus and R. Marcos: *Met. Res.*, 1999, **446**, 23.
11. J. A. Kubinski, T. Hurkmans, T. Trinh, W. Heischer, G. J. Vander Kolk, *Plating & Surf. Fin.*, 1999, **86**, (10), 20.
12. M. Koch and U. Eberbach: *Surf. Engg.*, 1997, **13**, (2), 157.
13. J. R. Smith, S. Breakspear and S. A. Campbell: *Trans Inst Met Fin.*, 2003, **81**, (2), B26.